Experimental investigation on material removal and brittle–ductile transition of SiC ceramics milling regarding milling force characteristic and tool wear

jian qiu (qiuj1981@163.com)
Shenyang Machine Tool (Group) CO., LTD

Renpeng Ge
Shenyang machine tool group CO. LTD.

tingchao han

Research Article

Keywords: SiC Ceramics milling, Brittle–ductile transition, Cutting force, Surface quality, Tool wear

Posted Date: March 9th, 2021

DOI: https://doi.org/10.21203/rs.3.rs-181143/v1

Experimental investigation on material removal and brittle–ductile transition of SiC ceramics milling regarding milling force characteristic and tool wear

Jian Qiu[1,2] Renpeng Ge[1] Tingchao Han[1]

1. State Key Laboratory of High-grade NC Machine Tools, Shenyang Machine Tool (Group) CO., LTD., Shenyang

2. National-Local Joint Engineering Laboratory of NC Machining Equipment and Technology of High-Grade Stone, Shenyang Jianzhu University, Shenyang 110168

Abstract：This research of SiC ceramics milling with diamond tool is paid attention to the milling mechanism and the cracks formation to found the brittle–ductile transition. The ductile material removal process of ceramics milling was discussed based on milling geometric models. Based on the material characteristics and fracture mechanics theory of SiC ceramics, the chip formation process and the brittle–ductile transition of ceramics milling were analyzed. The milling experiments of SiC ceramics were carried out, and the effect of cutting parameters on material removal mode was investigated. Based on milling forces, surface topography and chip morphology, the removal mechanism of ceramics milling was analyzed. Diamond tool wear on the material removal and milling forces during milling was investigated. Different methods were compared to identify the critical milling parameters of brittle–ductile transition, which can be used to recommend the milling parameters for crack control and high quality cutting.

Key words：SiC Ceramics milling; Brittle–ductile transition; Cutting force; Surface quality; Tool wear

1 Introduction

SiC ceramics is widely used in aerospace, automotive, electronics, optics and other fields for its advantages of high hardness and good wear resistance. The processing of SiC ceramics can be accomplished by diamond grinding which is the main machining method. Zhou [1] found the critical chip formation thickness and critical ductile-brittle transition thickness based on the mechanic deformation behavior of SiC. Zhang [2] investigated the influence of the dressing method of monolayer brazed diamond wheel on the material removal mechanism. In addition to the traditional grinding methods, SiC ceramics can also be removed by a variety of processing methods. Laser-assisted grinding is a promising method for cost-effective machining of hard and brittle materials, such as (RB)-SiC ceramics [3] and Al2O3 ceramics [4]. The assisting electrode machining is another practical and effective methods to machine SiC ceramics. Researchers like Rao [5] presented a research on surface characteristics for RB-SiC ceramics by electrical discharge diamond grinding. Liu [6] carried out a study on SiC ceramics with electrical resistivity of 500 Ωcm by electrical discharge milling to solve the problems of costly and inefficient by using common diamond grinding. Guo [7] studied the influence of the process parameters including polarity of electrode, peak current, pulse-on time and pulse-off time on material removal rate, side gap, and surface roughness. Naotake Mohri [8] provide a method with a copper electrode in sinking EDM or with brass wire electrode in WEDM using kerosene as working fluid to machine ceramics, which make the machining very easy. Sánchez [9] described the development of sinking and wire electro-discharge machining technology for ceramics as silicon infiltrated silicon carbide, which could obtain an excellent surface finish and high removal rates for the industrial application. Ultrasonic vibration machining is also a good processing method to solve the ceramics machining problems of high hardness, low efficiency, high cost and easy to break [10]. Zhao [11] revealed the mechanisms governing machined surface formation of hard brittle monocrystalline 3C–SiC in ultrasonic elliptical vibration-assisted diamond cutting by molecular dynamics simulations, which demonstrate the effectiveness of applying ultrasonic vibration of cutting tool in decreasing machining force and suppressing crack events. But, with the development of diamond cutting tools, the machining of SiC ceramics can also be carried out by diamond milling. It needs to overcome the difficulties of rapid tool wear and high processing cost, the poor surface quality control, and the low processing efficiency. Among them, the most important problem is that the hard and brittle property of ceramics is easy to produce cracks in the cutting process, which results in the decrease of cutting quality.

The hardness and brittleness of ceramics are relative concepts on the macro scale. When the cutting parameters are optimized, the cutting process can be improved to satisfy ductile material removal. The purpose of this research is to analyze the cutting mechanism of SiC ceramics using diamond tool on a machining center, to establish corresponding cutting models, to master the critical parameter interval of brittle-ductile transition, and to

* Corresponding author. Tel.: +86 024 25191396, Fax.: +86 024 25191670
E-mail address: qiuj1981@163.com (J. Qiu).

optimize cutting parameters, so as to achieve high efficiency and high quality. The cutting mechanism of brittle-ductile transition has received much attention over the past two decades, especially on the experimental and investigation research. Goel [12] performed an experimental study on diamond turning of single crystal 6H-SiC on an ultra-precision diamond turning machine to elucidate the microscopic origin of ductile-regime machining. They obtained fine surface finish better than any previously reported value on SiC while significant wear marks on the cutting tool was observed. Liang [13] performed an elliptical ultrasonic assisted scratching experiments and found material removal ratio in elliptical ultrasonic assisted grinding (EUAG) of mono crystal sapphire is increased in ductile–brittle transition region. It is prone to achieve ductile region with greater vibration amplitude in EUAG. Wang [14] presented an investigations of critical cutting speed on ductile-to-brittle transition mechanism by modelling and micrographs observation on chips, chip roots and finished surfaces. Simon [15] described an application of a "semi-elastic" machining method called shape adaptive grinding using an elastic tool combined with rigid pellets and super abrasives to finish aspheric mirror and reduce form error with no residual damage. And the mechanics driving brittle-ductile transition on finishing optical ceramic materials was more understood.

In addition to the research carried out by experimental methods, molecular dynamics studies have been conducted to investigate the atomicscale details of the cutting zone during the brittle-ductile cutting mode transition due to the difficulties in directly observing by experimental techniques [16]. The result verified by a plunge cutting experiment shows that tensile stress exists around the cutting zone and increases with undeformed chip thickness and finally induces brittle fractures.

2 Experiments

2.1 Experimental set-up

The cutting test was carried out on a NC machining center VMC850e manufactured by Shenyang Machine Tool Group. The machine tool and test equipment are shown in Fig. 1. The diamond milling tool was used for cutting slot cutting of SiC ceramics. And the cutting force, AE signals were recorded. The six component force dynamometer of Kistler 9265B, Kistler 5070 charge amplifier, and Dynoware data acquisition software were used for milling forces measurement. A microscope of Keyence vhx2000 was used to test tool wear, machining surface and chips, while a 3D profiler was used to measure the surface topography and roughness. The new tool is shown in Fig.1def.

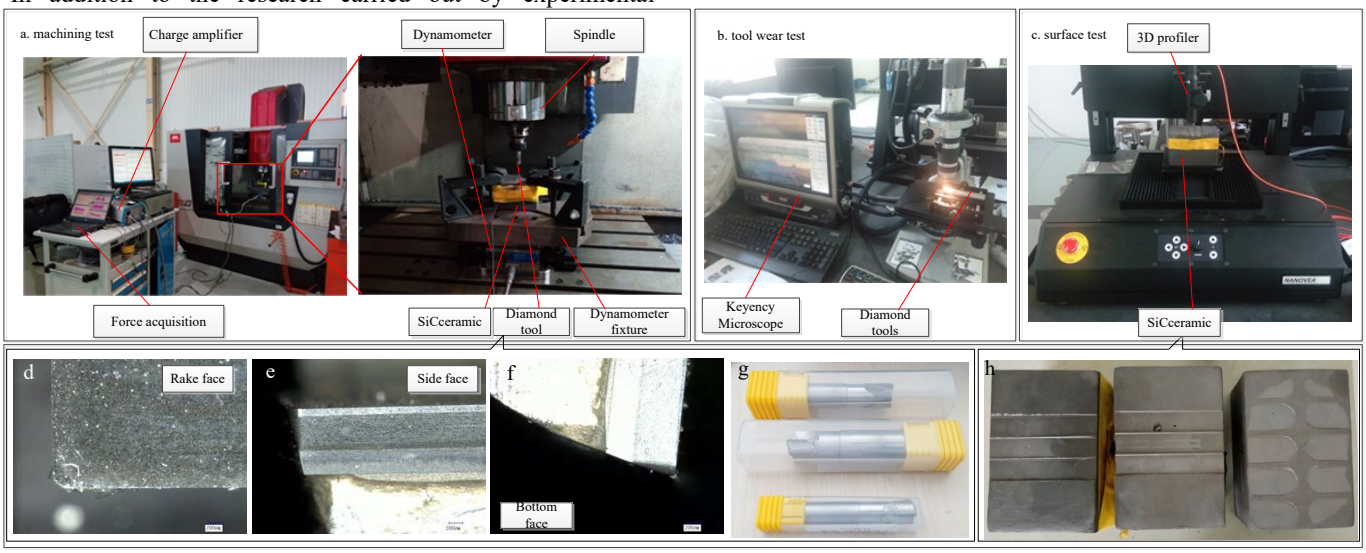

Fig. 1 Test of SiC Ceramics milling (a. machining test; b. tool wear test; c. surface tests; def. rake, side, and bottom faces of new tool; g. diamond tool; h. SiC workpiece)

2.2 Test workpiece and cutting tool

In the cutting test, the workpiece is SiC ceramic with size of 120 mm × 80 mm × 80 mm. The material properties of SiC ceramics and parameters of diamond tool are shown in Table 1.

Table 1 Material properties and tool parameters [17]

Material characteristics	Value
Fracture toughness K_c, MPa m$^{1/2}$	1.9
Hardness H, GPa	22
Elastic modulus E, GPa	347.01
Critical crack length Y_c, μm	0.895
Critical chip thickness h_{cis}, μm	0.01764
Tool characteristics	**Value**
material	Diamond tool
Tool angle	90°
Cutting edge angle	90°
Tool diameter	16
Tooth number	2
Inclined angle	0°

Edge shape	straight

2.3 Cutting test design

Single factor experiments were designed to test the cutting parameters region of brittle-ductile transition regarding the influences of cutting parameters and tool factors and machine tool specification. The cutting test was designed for tool full width milling. Exp. I was designed for single factor test of varied spindle speed corresponding to different cutting depths and single factor of varied feed rate. Exp.II using similar parameters with Exp. I was set for duplicate validation. Exp.III was designed for the effect of feed rate for different parameters range. Exp.IV was designed for the effect of machine tool specification. All the cutting parameters are shown in Table 2.

Table 2 List of cutting parameters

Exp.I-effect of spindle speed and cutting depth and feed rate (VMC850e)						
n	Δn	f_z	Δf_z	a_p	Δa_p	MRR
1000-4000	1000	0.01	-	0.1	-	32-128
1000-4000	1000	0.01	-	0.2	-	64-256
1000-4000	1000	0.01	-	0.15	-	48-192
3000	-	0.005-0.02	0.005	0.1	-	48-192
2000-4000	1000	0.01	-	0.1	-	64-128
2000-4000	1000	0.01	-	0.2	-	96-256
Exp.II-effect of single cutting parameter (VMC850e)						
n	Δn	f_z	Δf_z	a_p	Δa_p	MRR
1000-4000	1000	0.01	-	0.15	-	48-192
3000	-	0.005-0.02	0.005	0.1	-	48-192
1000	-	0.01	-	0.05-0.2	0.05	16-64
Exp.III -effect of feed (VMC850e)						
n	Δn	f_z	Δf_z	a_p	Δa_p	MRR
2000	-	0.005-0.025	0.005	0.1	-	40-200
Exp.IV-effect of machine tool specification (VMC1100b)						
n	Δn	f_z	Δf_z	a_p	Δa_p	MRR
1000	-	0.005-0.025	0.005	0.1	-	20-100
2000	-	0.005-0.025	0.005	0.1	-	40-200
3000	-	0.005-0.025	0.005	0.1	-	60-300

*Δn, Δf_z and Δa_p are the increasing steps of spindle speed, feed rate and cutting depth.

3 Results and Discussion

3.1 Forces characteristics of SiC ceramics milling

By analyzing the combination of cutting forces in X and Y directions with cutting parameters of n=4000 r/min, f_z=0.01 mm/z, a_p=0.1 mm, it can be found that the X-Y plot of cutting forces is variable. The range of forces trajectory at the early cutting stage is large and discrete. In the later stage of cutting, the range of the trajectory in Y axis is larger.

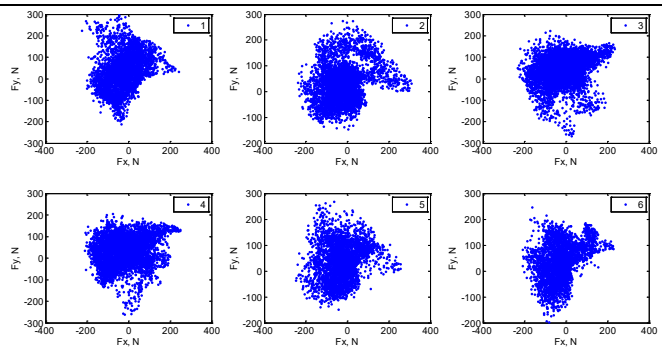

Fig. 2 X-Y plot of cutting forces

Fig. 3 shows the average cutting forces comparisons before and after tool wear in the varied feed rate cutting when n=3000 r/min, a_p=0.1 mm. It is found that the cutting forces with worn tool are larger than the cutting forces of unworn tool. And the cutting modes before and after tool wear are different. For the worn tool, cutting mode is brittle when the feed rate per tooth exceeds 0.015 mm/z and the cutting forces decrease significantly. It is found the cutting forces of SiC ceramics depend on the material removal mode. When the material removal modes are different, and even both brittle removal but different proportion of brittle-ductile removal, the cutting forces are different.

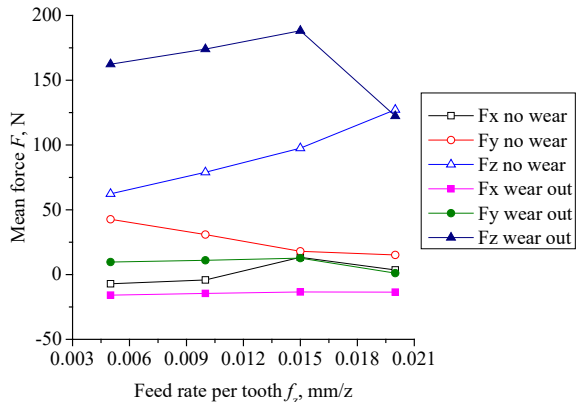

Fig. 3 Cutting forces distribution in varied feed milling with the same parameter before and after tool wear

Some typical cutting force signals are shown in Fig. 4 in time domain and frequency domain. The cutting forces have the following characteristics:

(1) The cutting force in the Z axial direction is much larger than the other two axial forces in the SiC ceramics cutting. In metal cutting, the cutting load has little effect on the cutting edge in the direction of the Z axis, and the cutting force in the Z axial direction is not sensitive to the cutting parameters. In the SiC ceramics cutting, the removal of material includes brittle fracture and ductile shear. When the brittle fracture occurs, the material removal volume does not continue increase as the material removal, but keep the removal volume almost unchanged because of the powder chip of ceramics. This can be proved by evidence of forces do not increase significantly with the increasing of cutting parameters, especially the cutting forces in the feed direction and its orthogonal direction. In particular, when

the cutting force is close to the peak value of each tool tooth cycle, the force will be superimposed by the generation of brittle fracture. But, with the increasing of feed rate beyond the region of brittle-ductile transition, the proportion of brittle removal increases, and the cutting forces reduce.

(2) It is concluded that the increasing of spindle speed will soften the ceramics to improve the cutting load. One evidence is that the sinusoid-like forces signals are changed more stable and smoother from 2000 r/min to 4000 r/min, as shown in Fig. 4abc.

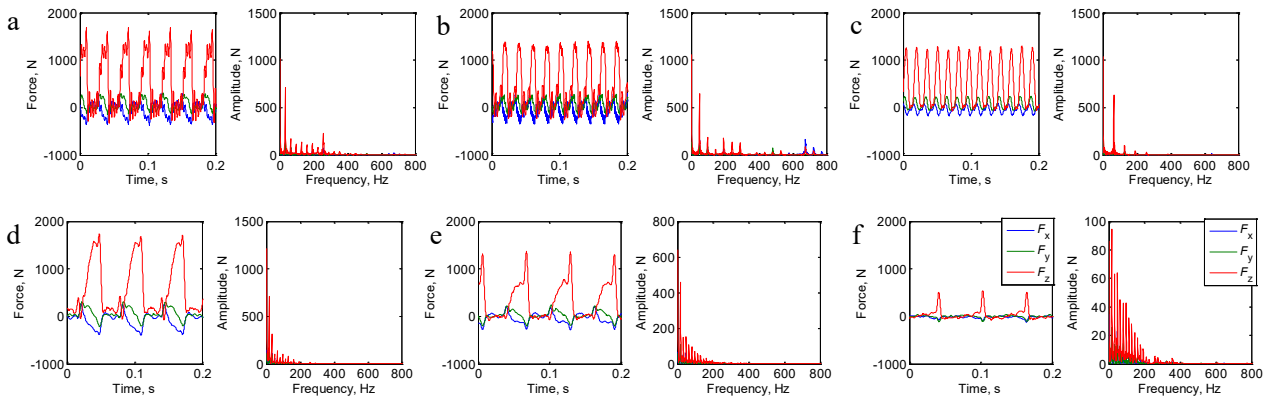

Fig. 4 Time and frequency domain signals of cutting forces of worn tool. (a) n=2000 r/min, f_z=0.01 mm/z, a_p=0.15 mm. (b) n=3000 r/min, f_z=0.01 mm/z, a_p=0.15 mm. (c) n=4000 r/min, f_z=0.01 mm/z, a_p=0.15 mm. (d) a_p=0.2 mm, n=1000 r/min, f_z=0.01 mm/z. (e) a_p=0.15 mm, n=1000 r/min, f_z=0.01 mm/z. (f) a_p=0.1 mm, n=1000 r/min, f_z=0.01 mm/z.

(3) Taking the cutting force of Z direction as an example, the varied feed cutting tests with the same cutting parameters are repeated after a series of cutting tests. Because of tool wear, the cutting force increases, and the cutting force signals in the same tooth cycle become disordered with many frequency components, as shown in Fig. 5. Compared with the smooth cutting force signals of no wear tool, more peaks appear, and the most prominent peak value in time domain of worn tool signals becomes steep.

No matter the tool is worn or not, the frequency components of the cutting force signals are the rotation frequency of the cutter teeth, but more frequency components appear in the high frequency range of the worn tool signals. In the frequency range of more than 500 Hz, there are almost no frequency components of the no wear signals, while the peak values in the high frequency range of worn tool signals from feed rate of 0.005 mm/z to 0.015 mm/z are still very large, as shown in Fig. 5. When the feed rate increases from 0.015 mm/z to 0.02 mm/z, the cutting force is reduced, and the high frequency components in frequency domain disappear, which means the material removal mode changes from ductile removal to brittle removal.

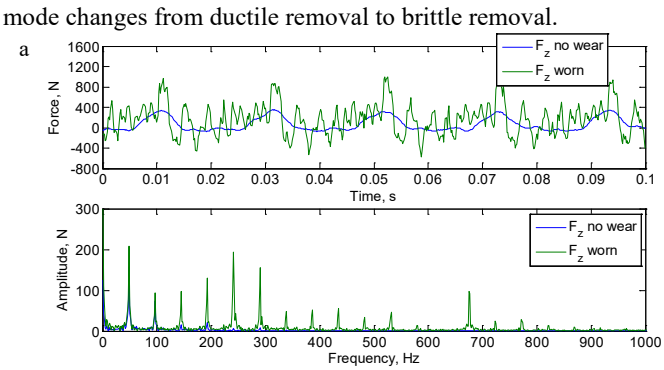

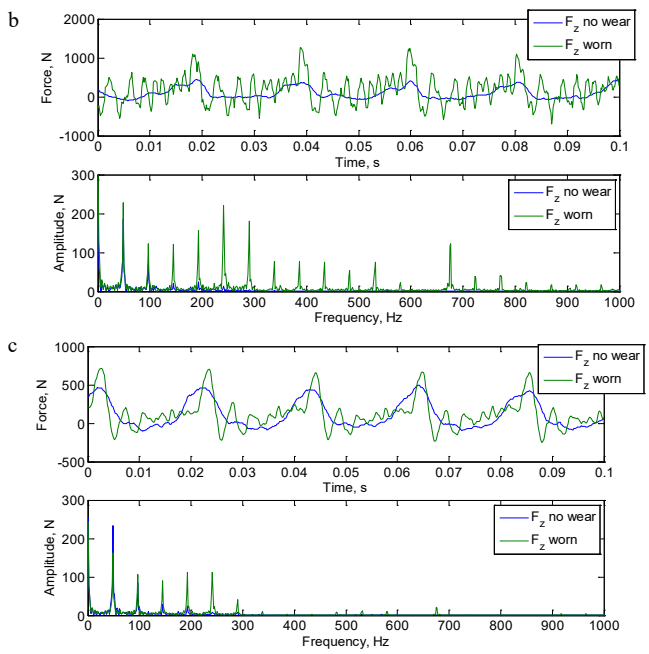

Fig. 5 Force signals before and after tool wear in varied feed rate cutting (n=3000 r/min, a_p=0.1 mm). (a) f_z=0.005 mm/z. (b) f_z=0.015 mm/z. (c) f_z=0.02 mm/z.

Fig. 6 shows the comparison of the two varied feed rate cutting tests with the same parameters. When the tool is not worn, the frequency components and peak values in frequency domain corresponding to feed rate of 0.005, 0.015, and 0.02 mm/z are very close. The peak values of worn tool in frequency domain are larger than that of unworn tool. A larger feed rate corresponds to a larger amplitude. Both of the peak values of the first 2 orders frequencies of no wear tool and worn tool in frequency domain are larger. The peak values of worn tool near the 5th harmonic and 14th harmonic are larger.

For force signals in frequency domain using worn tool in the

ductile removal range, the number of frequency components at feed rate of 0.015 mm/z is more than that of 0.005 mm/z. The peak values of worn tool with feed rate of 0.015 mm/z are greater than that of 0.005 mm/z. And when the feed rate exceeds 0.015 mm/z to 0.02 mm/z, the frequency of worn tool, the number of the high frequency components of worn tool reduce, and the peak values decrease obviously. The peak frequency at 0.02 mm/z is obviously smaller than that of the other two parameters, and the difference between the first 3 orders is larger. These indicate that the material removal mode has changed.

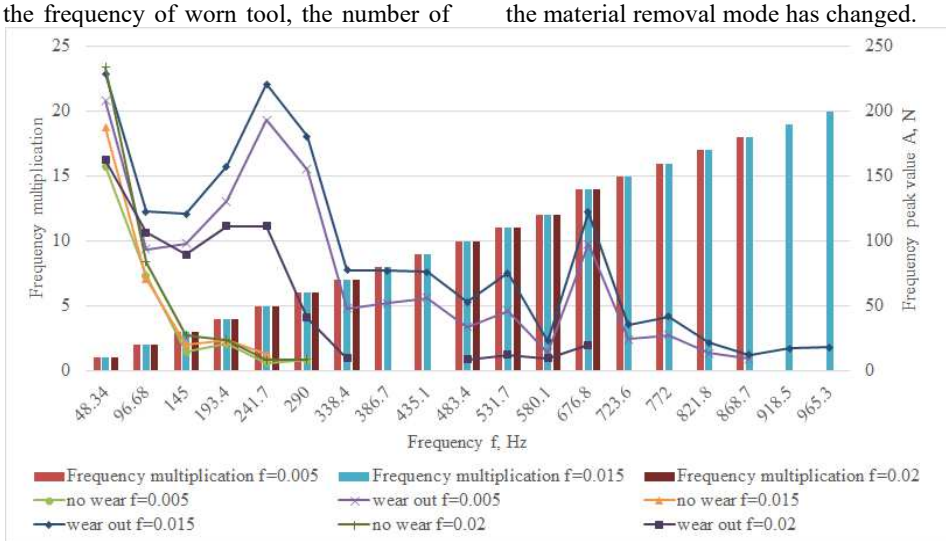

Fig. 6 Force rotation frequency of tool before and after wear

Fig. 7 Tool surfaces. New tool. (a) Rake face 100×. (b) Flank face 100×. (c) Bottom edge 100×. Worn tool. (d) Rake face 50×. (e) Flank face 20×. (f) Bottom face 50×.

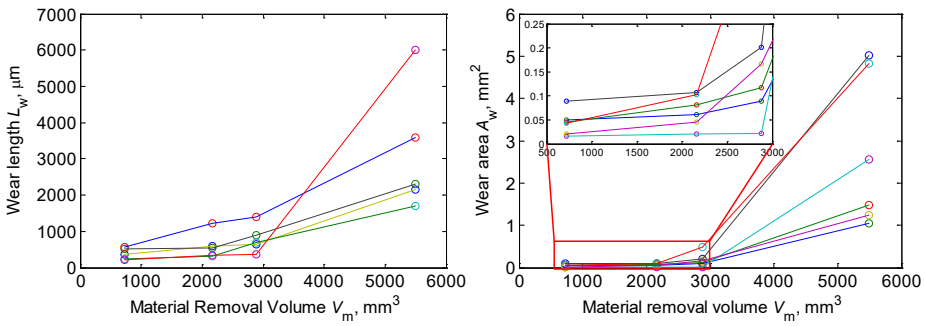

Fig. 8 Tool wear length and wear area with material removal volume

(4) Fig. 9 shows the comparison of surface integrity and chip form between relative large cutting depth and relative large spindle speed and feed rate. The results show that the processing with larger cutting depth tends to brittle removal when the parameters are n=1000 r/min, f_z=0.01 mm/z, a_p=0.2 mm. Evidence shows that the region B in Fig. 9ab has a lot of tiny cracks on the machined surface. When the cutting depth decreases and relative larger spindle speed and feed rate with the parameters of n=3000 r/min, f_z=0.015 mm/z, a_p=0.1 mm, the machined surface shows no obvious micro cracking, such as region C in Fig. 9f. And both sides of the groove shoulders are integrity and no material spalling, as shown in Fig. 9d. The chips are powder chips with the same morphology as Fig. 9e shows. The chips produced at the two sides of the groove shoulders are block chips formed by brittle fracture as shown in Fig. 9c. Evidence of the forming of block chips is that the crack propagation in the cutting process is very easy to cause massive spalling due to the low bonding strength of SiC ceramics, especially at the shoulder of cutting groove, as region A shown in Fig. 9a. But most of the chips produced in SiC ceramics cutting

are powder chips, as shown in Fig. 9e.

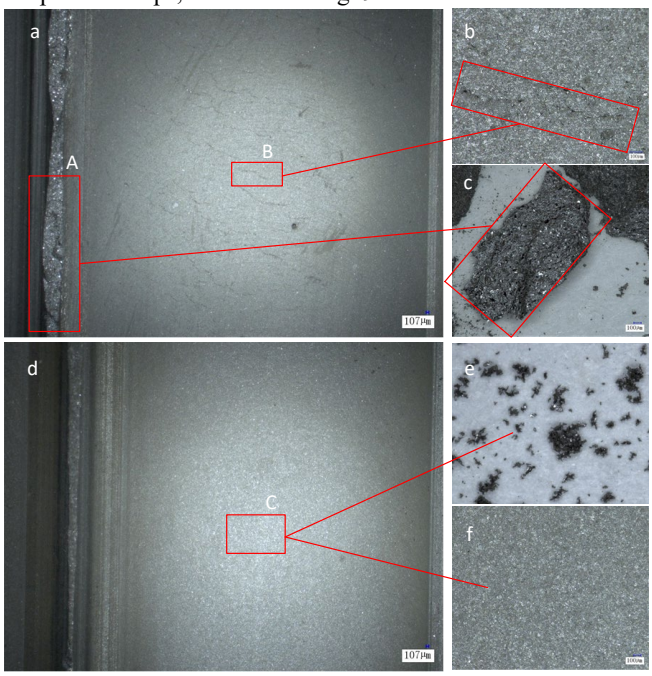

Fig. 9 Surface integrity. (abc) poor quality surface with material spalling induced by crack (n=1000 r/min, f_z=0.01 mm/z, a_p=0.2 mm). (def) high quality surface (n=3000 r/min, f_z=0.015 mm/z, a_p=0.1 mm)

(5) In each tooth rotation cycle, when each tool tooth rotates close to the position of the maximum chip thickness, the material removal will change from ductile removal to brittle removal. It can also be considered the material removal will be combined with brittle collapse on the basis of ductile removal. Thus, a small amount exciting force is produced on the tool section, as shown in Fig. 4ad. The tool surfaces of new tool and worn tool are shown in Fig. 5. Moreover, the cutting of ceramics will not break in some parameters, and the cutting forces are stable, as shown in Fig. 4c.

The wear of the two cutting edges at the positions of tool rake face, main cutting edge, secondary cutting edge and tool tip radius increase with the increase of material removal volume, as shown in Fig. 8. A single tooth of tool will be first worn or damaged. Then the tool rotation is unbalance. When the wear continues, the two teeth are worn or damaged. With the increasing of material removal volume, the cutting edges are worn into arc shape. The cutting of brittle materials is easy to cause cracks. After material removal volume exceeds 3000 mm^3, tool wear increases significantly.

3.2 Surface topography and roughness

Surfaces in three cutting tests with the same material removal rate of 192 cm^3/min and different cutting parameters in Table 2 are compared in order to determine the effect of cutting parameters on the brittle-ductile transition [18]. Some researchers also used 3D profilometer [19] or SEM [20] to study the brittle–ductile transition of brittle materials cutting.

The cutting mechanism of SiC ceramics is different from plastic shear in metal cutting, but also different from the usual brittle fracture in high brittle material removal. Brittle fracture accompanies with ductile deformation in the milling process of ceramics, and the proportion of the two kinds of material removal mode is uncertain with the different processing conditions and material properties. The order sensitive factors in the selected parameters on brittle-ductile processing surface of SiC ceramics is f_r>n>a_p. It is as far as possible to choose a parameter combination of smaller feed rate and relative larger cutting depth in the same material removal rate. When the cutting parameters especially feed rate decreases, an increase in ductile removal proportion is presented.

The surface roughness S_a and S_q increase linearly with the spindle speed increasing from 1000 r/min to 3000 r/min. When the spindle speed increases to 4000 r/min, the surface roughness increases, as shown in Fig. 10(a). The surface skewness coefficient increases and the kurtosis coefficient decreases monotonically with the spindle speed increasing from 1000 r/min to 3000 r/min while the skewness coefficient and kurtosis coefficient of surface greatly reduces when the spindle speed increases to 4000 r/min, as shown in Fig. 11 (a).

In the cutting test of varied cutting depth, S_q, S_a, S_{sk} increase with cutting depths changing from 0.05 mm to 0.15 mm (, while S_{ku} decreases, as shown in Fig. 10 (b) and Fig. 11(b). When the cutting depth increases to 0.2 mm, the tendencies of S_q, S_a, S_{sk} and S_{ku} are changed.

In the varied feed rate cutting test, the surface roughness and the skewness coefficient increase linearly with the feed rate increases from 0.005 to 0.015 mm/z, while the kurtosis coefficient decreases linearly. When the feed rate reaches 0.02 mm/z from 0.015 mm/z, the tendencies of the surface roughness indexes of S_q, S_a, S_{sk} and S_{ku} change to the opposite position, as shown in Fig. 10(c) and Fig. 11(c).

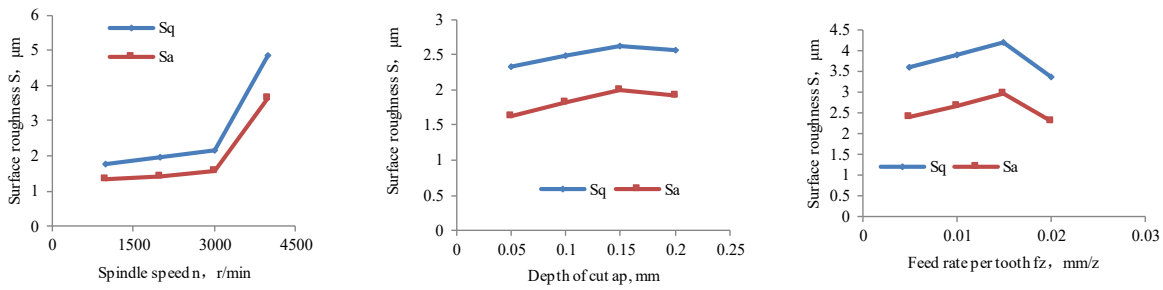

Fig. 10 Surface roughness S_a and S_q obtained by (a)varied speed test (f_z=0.01 mm/z, a_p=0.15 mm). (b) varied cutting depth test(n=1000 r/min and f_z=0.01). (c) varied feed test (n=3000 r/min and a_p=0.1).

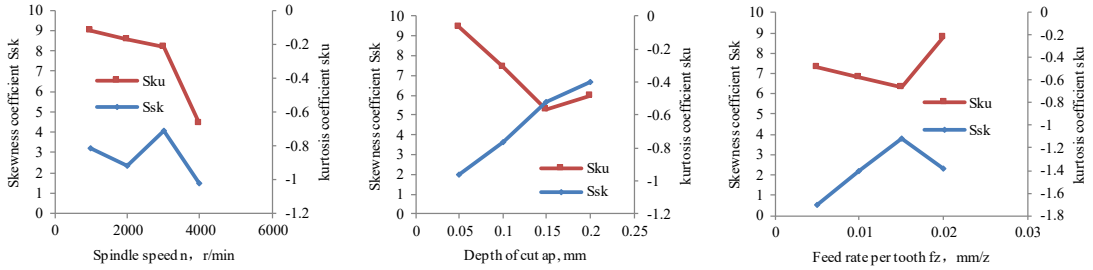

Fig. 11 Surface skewness coefficient S_{sk} and kurtosis coefficient S_{ku} obtained by (a)varied speed (f_z=0.01 mm/z, a_p=0.15 mm). (b) varied cutting depth (n=1000 r/min and f_z=0.01). (c) varied feed (n=3000 r/min and a_p=0.1).

Evidence shows that the material removal mode changes from ductile removal to brittle removal in this interval of spindle speed from 3000 r/min to 4000 r/min, cutting depth from 0.15 mm to 0.2 mm and feed rate from 0.015 mm/z to 0.02 mm/z.

4 Analysis of brittle-ductile transition of milling

4.1 Chip formation analysis based on stress-strain

The chip formation of metal cutting is simplified as shown in Fig. 12ab. Metal materials in the tool tip is under the action of the compression stress. Due to the different movement directions of the chip and the machined surface, the chip separation area I that contacts with the tool's rake face mainly bears tensile stress from material removal, while the second main stress area II is mainly subjected to the compressive stress produced by chip bending, as shown in Fig. 12b2. The chips slip along the tool's rake face, and break apart after curling to fracture strength. The morphology of chips is related to material properties and cutting parameters. Sawtooth chips (Fig. 12b3) and curling chips (Fig. 12b4) can be formed under different conditions. If the material is brittle, the sawtooth chips are prone to fracture and form powder chips, such as cast iron.

The transition of ceramics from ductile cutting to brittle cutting can be explained as:

When the cutting thickness does not exceed the critical value of brittle-ductile transition, the material cutting mode are mainly ductile removal. The deformation of ceramics materials in the tool tip is similar to metal. The brittle material is forced under the action of the compression stress in the separation area I and the second main stress area II in Fig. 12c2. Subsequently, the ceramics materials at the tool tip fracture, and the chips separate from workpiece along the rake surface of cutting tool. With the continuous increasing of stress in region I and region II, the chips are gradually stripped from the ceramics workpiece gradually. And the separated chips are broken into powder chips under the influence of extrusion stress in region II. The existence of ceramic chips is probabilistic, and the Webb distribution function can be used to describe the fracture of a chip, as shown in Eq.(1).

$$f_c(\sigma) = 1 - \exp\left[-\left(\frac{\sigma}{\sigma_0}\right)^m \int_v \left(\frac{\sigma'}{\sigma}\right)^m dv\right] \tag{1}$$

where, $f(\sigma)$ is fracture probability; m is Webb coefficient, the greater the value, the smaller the probability of fracture; σ_0 is characteristic stress; σ and σ' are the internal stress and its maximum value.

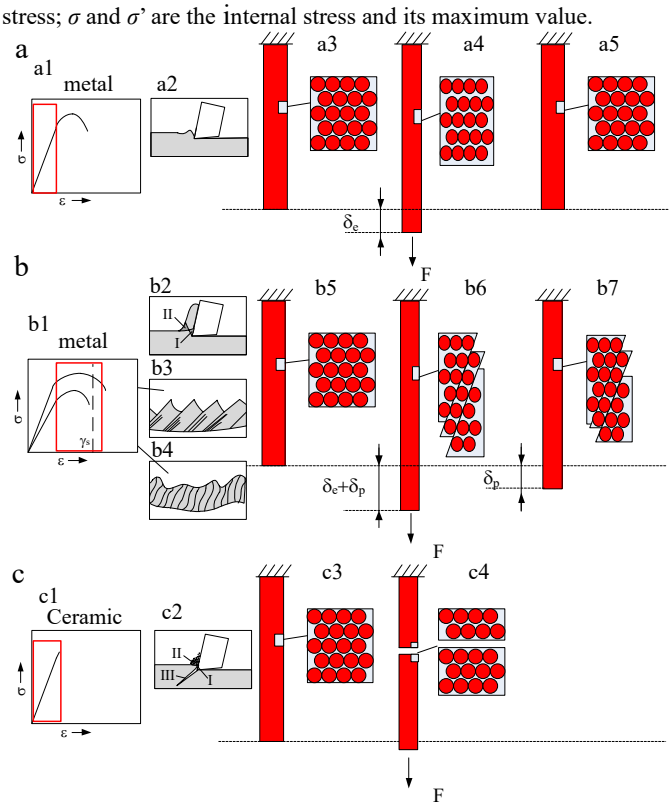

Fig. 12 Chip formation mechanisms and stress-stain comparison of metal and ceramics. (a) elastic deformation of metal. (b) plastic deformation of metal. (c) brittle deformation of ceramics. (F is force, δ_e and δ_p are the elastic deformation and plastic deformation.)

The critical load required for the crack initiation of ceramics with respect to the toughness and hardness of the ceramics material is given in Eq.(2), and the crack length of ceramics cutting is present in Eq.(3) [13].

$$P = \lambda_0 \frac{K_c^{\,4}}{H^3} \tag{2}$$

$$l = \mu_0 \frac{K_c^{\,2}}{H^2} \tag{3}$$

where, λ_0 and μ_0 are geometric constants related to materials properties; P is critical load, kW; l is crack length, μm; K_c is fracture toughness, which is a characterization to resistance material fracture; H is material's hardness.

The critical chip thickness of ceramics cutting can be extended from the critical indentation size in the indentation fracture mechanics [21] as shown in Eq.(4).

$$h_{CIS} = K\frac{E}{H}\left(\frac{K_c}{H}\right)^2 \tag{4}$$

where, E is elastic modulus, GPa, K is the coefficient relate to critical chip thickness.

When the cutting thickness beyond the critical value of brittle-ductile transition, cutting of brittle materials produces significant volume expansion before broken and chip formation. The strain produced by ceramic cutting under steady load tends to be inelastic and non-recoverable as Fig. 12c1 shows. It is difficult to describe the chip shape in the deformation of ceramic cutting. The chip geometric of ceramics is different from the undeformed chip with no broken calculated in Eq. (1). The undeformed chip will crack under the deformation force as shown in Fig. 12c2. These cracks tend to expand, causing chips to break suddenly in a very small form and further to fracture. Therefore, the cutting of ceramics will cause chips to break, and the broken chip will form powder like crystalline particles.

When the cutting thickness beyond the critical value, it generates crack in the process of chip separation, the cracks on the interface of chip-workpiece in the stress region I are tensile stress crack, and the cracks produced on the machined surface in the stress region II are compressive stress cracks. The tensile stress cracks have great influence on the machined surface for their special position, while the compressive stress cracks tend to crush the ceramics material. The appearance of cracks will accelerate the process of material removal, and the material removal mode will change from ductile to brittle. Cracks will extend to the machined surface easily to form machined surface defects, as shown in Fig. 12c2 III. The cutting process of ceramics is a combination of ductile removal and material removed with micro fracture. Tool geometry and cutting parameters have influence on the morphology of ceramics removal. The absolute ductile deformation occurs only in the processing condition [22] below the critical values.

Explain from the view of, the metal material is deformed by the loading force F (Fig. 12a4) in the elastic deformation stage as shown in stress-strain curve of Fig. 12a1. When the force F is unloaded, the material rebounds almost without deformation (Fig. 12a5). In the stage of plastic deformation in Fig. 12b1, the material deforms under the action of force F (Fig. 12b6). When the force F is unloaded, the material is partly rebound, but the overall deformation is larger than before loading (Fig. 12b7). The geometric of metal will change before fracture, and some phenomena can be used to predict fracture. But the ceramics will hardly deform before break, the fracture will happen in a flash and randomness difficult to predict. From the stress-strain curve of ceramics material, it is approximately consistent with Hooke's law when the stress produced by the loading force F is small, as shown in Fig. 12c1, and the material will not yield as there is no yield stage in the curve. When the loading force is beyond the critical force, material broken in the stage almost with no plastic deformation but break (Fig. 12c4). And the elongation is almost negligible.

4.2 Critical stability interval of brittle-ductile transition

Lawn and Marshall [21] proposed an empirical relationship model between the critical load and the crack length on the machined surface. The ductile material removal model of SiC ceramics milling with straight diamond tool can be seen as shown in Fig. 13. When the chip thickness h reaches a critical thickness of h_c, the material begins to be removed from ductile to brittle. If the chip thickness is less than the critical thickness, material removal mode can be considered as ductile removal. Conversely, it tends to brittle removal and initial cracks will generate. When the cracks generate, it will extend to the ceramics surface and result in processing defective.

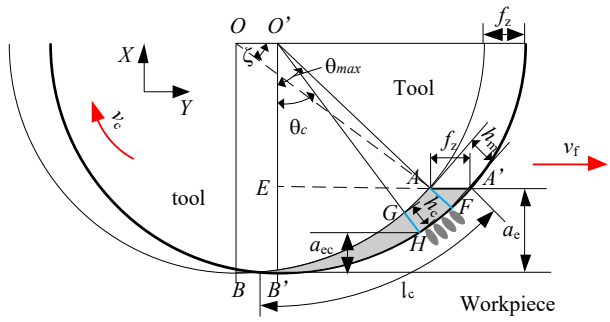

Fig. 13 Milling geometry model

The maximum undeformed chip thickness and chip length in the milling process can be seen in Eq.(5)[23].

$$\begin{cases} h_{\max} = 2f_z\sqrt{\dfrac{a_e}{D}} - \dfrac{f_z^2}{D} = f_z \sin\theta_{\max} \\ l_c = \sqrt{a_e D} \end{cases} \tag{5}$$

where, $h_{\max}$ is the maximum undeformed chip thickness, mm; f_z is the feed rate per tooth, mm/z; a_e is the cutting width, mm; D is the tool diameter, D=2R, and R is the radius, mm; l_c is the chip length, mm; The angle corresponding to the maximum undeformed chip thickness $\theta_{\max} = \arccos\left(\dfrac{D-2a_e}{D-2h_{\max}}\right)$.

When the undeformed chip thickness h_m is equal to the critical thickness h_c, the critical feed rate per tooth can be obtained, as shown in Eq.(6).

$$f_{zc} = h_c\sqrt{\frac{R}{2a_e}} \tag{6}$$

The conditions to achieve the ductile cutting of SiC ceramics

[17,24] for ideal surface are $h_{\max} \le h_c$.

According to the second equation in Eq.(5), the undeformed chip thickness corresponding to any point of the chip during tool cuts into the workpiece can be expressed as shown in Eq. (7) [25].

$$h_{\mathrm{m}} \approx f_z \sin\theta \tag{7}$$

When h_{m} reaches the critical chip thickness h_{c}, the depth of cut a_{ec} corresponding to the undeformed chip thickness greater than h_{c} will cause cracks. The critical feed rate and critical radial cutting depth corresponding to the critical chip thickness are shown in Eq.(8).

$$\begin{cases} f_{zc} = \dfrac{h_c}{\sin\theta_c} \\ a_{ec} = \dfrac{D(1-\cos\theta_c)}{2} + h_c\cos\theta_c \end{cases} \tag{8}$$

The critical rotation angle of tool can be expressed as Eq.(9):

$$\theta_c = \arcsin\left(h_c / f_z\right) \tag{9}$$

Therefore, it can be concluded that the cutting condition without crack is that the maximum undeformed chip thickness does not exceed the critical chip thickness.

The cutting parameters affecting chip thickness include feed rate and radial cutting depth. Accordingly, as long as these two parameters are controlled within the critical value, ductile cutting can be achieved. The corresponding feed rate conditions and radial cutting depth conditions are shown in Eq.(10) and Eq.(11).

Feed rate conditions:

$$f_z < f_{zc} = \frac{h_c}{\sin\theta_{\max}} \tag{10}$$

where, $\theta_{\max} = \arccos\left(\dfrac{D-2a_{\mathrm{e}}}{D-2h_{\max}}\right)$.

Radial cutting depth condition:

$$a_e < a_{ec} = \frac{D(1-\cos\theta_c)}{2} + h_c\cos\theta_c \tag{11}$$

where, $\theta_c = \arcsin\left(h_c / f_z\right)$.

The relationship between cutting parameters such as feed rate and radial depth of cut and ductile – brittle transition is concluded in Fig. 14.

(1) When the feed rate and depth of cut are much smaller than the critical value, the interaction between abrasive grain and workpiece is shown as ploughing.

(2) When the feed rate and depth of cut are smaller than the critical value but not much smaller, the material are removed as ductile removal.

(3) When the feed rate is larger than the critical depth of cut and critical feed rate, the cutting cracks will generate. The mechanism of crack formation during ceramics cutting is the same as that of indentation fracture mechanics.

(4) When the feed rate and cutting depth satisfy that one of the parameters is smaller than the critical value and the other is higher than the critical value, brittle and ductile removal exist simultaneously. In addition, when any parameter is greater than the critical value, the material removal includes brittle removal thickness and plastic removal thickness. The fracture of ceramics materials is a combination of material properties and external loads, and undeformed chip morphology.

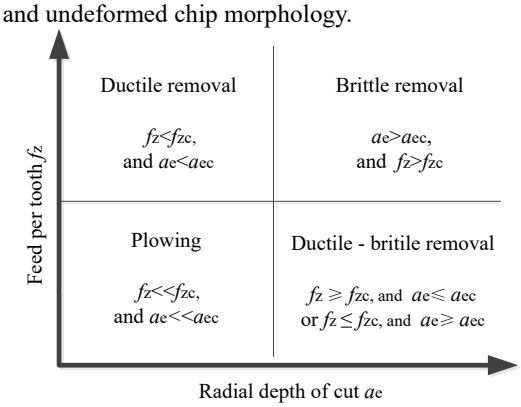

Fig. 14 Critical condition of brittle-ductile cutting transition

4.3 Determination of brittle-ductile transformation region

The ceramics cutting generally have different degrees of micro cracks appear [26,27]. The fracture strength of brittle materials does not depend on the number of microcracks, but depends on the length and depth of microcracks. When the crack size exceeds a certain value, it will expand rapidly.

Table 3 shows the tendency of material removal mode transition with cutting parameters increasing according to the experimental data. With the increasing of spindle speed, cutting depth and feed rate, the effect of material strain hardening increases and strain softening decreases. As a result, the material removal mode changes from ductile to brittle.

Table 3 Tendency of material removal mode transition with cutting parameters increasing

Parameter increase	Strain hardening	Strain softening	Material removal mode transition
Spindle speed 1000 to 4000	↑	↓	ductile→brittle
Cutting depth 0.05 to 0.2	↑	↓	ductile→brittle
Feed rate 0.005 to 0.02	↑	↓	ductile→brittle

Table 4 gives a comparison of the determination of the brittle-ductile transition region of SiC ceramics obtained by surface detection and processing signals. The critical interval of feed rate is 0.015 mm/z - 0.02 mm/z. The critical interval of cutting depth is 0.15 mm - 0.2 mm, and the cutting depth will lead to material breakage when the tool wear to a certain extent, such as less than 0.05 mm. Spindle speed in the interval of 3000-4000 r/min shows a slight change, but combined with other means of analysis, it cannot clearly determine the critical interval of spindle speed.

Table 4 Comparison of different ways for the determination of brittle-ductile transformation region of SiC ceramics machining

Parameters	Force	Roughness	Micro surface	Chip
Spindle speed	Not obvious	3000-4000	Not obvious	-
Cutting depth	Not obvious	0.15-0.2	≤0.1, ≥0.2	0.2
Feed rate	0.015-0.02	0.015-0.02	0.015-0.02	Not under 0.15

5 Conclusion

(1) An experimental study using diamond tool for SiC ceramics milling was carried out. It is found that the brittle–ductile transition of SiC ceramics cutting is existed. Better surface integrity of milling ceramics can be controlled in the ductile cutting, while surface defects such as cracks, spalling of materials, or pores can be found on the brittle removal surfaces.

(2) The proportion of the two kinds of material removal mode will determine material removal difficulty and surface quality. The cutting is controlled in a ductile removal mode if the undeformed chip thickness does not exceed the critical size of the ceramics fracture. The proportion of the brittle failure of ceramics milling can be reduced with the decreasing of feed rate, spindle speed and cutting depth. The critical parameter interval of feed rate in SiC ceramics milling is 0.015 mm/z - 0.02 mm/z, while the critical cutting depth is 0.15 mm - 0.2 mm.

(3) It is found that the cutting force in Z axial direction is the main cutting force. The cutting force of brittle materials is related to the proportion of brittle-ductile removal. The wearing tool is easy to cause brittle removal, where the signal of cutting force in frequency domain has more frequency related to spindle rotation. The cutting process is usually accompanied by the fracture of ceramics materials, chip spalling, and tool impacting. With the increasing of cutting volume, the tool edges are worn into arc shape. The wear area increases sharply when material removal volume exceeds 3000 mm^3.

Acknowledgement

This work is supported by Natural Science Foundation of Liaoning Province in China（2015010109-301）, National-Local Joint Engineering Laboratory of NC Machining Equipment and Technology of High-Grade stone SJSC-2015-11, China. The authors would like to express their appreciation to the agencies.

Declarations

-Ethical Approval: This work has no potential conflicts of interest. This work has no research involving Human Participants and/or Animals.

-Consent to Participate: Not applicable.

-Consent to Publish: Not applicable.

-Authors Contributions: Jian Qiu: Conceptualization, Methodology, Formal analysis, Test Design, Data Analysis, Supervision, Visualization, Discussion, Writing- Original draft preparation. Renpeng Ge: Test Validation, Sensor prepare, Data Record. Tingchao Han: Test Validation, Sensor prepare, Data Analysis.

-Funding: This work was supported by [Natural Science Foundation of Liaoning Province in China] (2015010109-301) and [National-Local Joint Engineering Laboratory of NC Machining Equipment and Technology of High-Grade stone, China] (SJSC-2015-11).

-Competing Interests: The authors declare that they have no known competing financial interests or personal relationships that could have appeared to influence the work reported in this paper.

-Availability of data and materials: All allowed data has been provided in the manuscript.

References

[1] Z. Wenbo, S. Honghua, D. Jianbo, Y. Tengfei, Z. Yihao, Numerical investigation on the influence of cutting-edge radius and grinding wheel speed on chip formation in sic grinding, Ceram. Int. 44 (2018) 21451-21460.

[2] K. Zhang, H. Su, W. Xu, Influence of plate wheel dressing of monolayer brazed diamond wheel on material removal mechanism in SiC grinding, Journal of Nanjing University of Aeronautics 8L Astronautics 46(5) (2014) 732-737.

[3] Z. Li, F. Zhang, X. Luo, W. Chang, Y. Cai, W. Zhong, Material removal mechanism of laser-assisted grinding of rb-sic ceramics and process optimization, J EUR CERAM SOC 39 (2019) 705–717.

[4] C. W. Chang, C. P. Kuo. An investigation of laser-assisted machining of Al2O3 ceramics planning, Int. J. Mach. Tool Manu. 47(3–4) (2007) 452-461.

[5] X. Rao, F. Zhang，L. Liu, Surface characteristics for RB-SiC ceramics by electrical discharge diamond grinding, Optics and Precision Engineering 24(9) (2016) 2192-2199.

[6] Y. H. Liu, R. J. Ji, Q. Li, L. Yu, X. Li, An experimental investigation for electric discharge milling of sic ceramics with high electrical resistivity, J. Alloy Compd. 472(1-2) (2009) 406-410.

[7] Y. F. Guo, Y. R. Feng, L. Wang, Experimental investigation of edm parameters for zrb2-sic ceramics machining, Procedia CIRP 68 (2018) 46-51.

[8] N. Mohri, Y. Fukuzawa, T. Tani, N. Saito, K. Furutani, Assisting electrode method for machining insulating ceramics, CIRP Ann-Manuf. Techn. 45(1) (1996) 201-204.

[9] J. A. Sánchez, I. Cabanes, L. N. L. D. Lacalle, A. Lamikiz, Development of optimum electrodischarge machining technology for advanced ceramics, Int. J. Adv. Manuf. Tech. 18(12) (2001) 897-905.

[10] J. Cao, M. Nie, Y. Liu. Ductile-brittle transition behavior in the ultrasonic vibration-assisted internal grinding of silicon carbide ceramics, Int. J. Adv. Manuf. Tech. 96 (2018) 9-12.

[11] L. Zhao, J. J. Zhang, J. G. Zhang, A. Hartmaier, Atomistic investigation of machinability of monocrystalline 3c-sic in elliptical vibration-assisted diamond cutting, Ceram. Int. (2020) In Press.

[12] S. Goel, X. Luo, P. Comley, R. L. Reuben, A. Cox, Brittle–ductile transition during diamond turning of single crystal silicon carbide, Int. J. Mach. Tool Manu. 65(2) (2013) 15-21.

[13] Z. Liang, X. Wang, Y. Wu, Experimental study on brittle - ductile transition in elliptical ultrasonic assisted grinding (euag) of monocrystal sapphire using single diamond abrasive grain, Int. J. Mach. Tool Manu. 71(8) (2013) 41-51.

[14] B. Wang, Z. Liu, G. Su, Investigations of critical cutting speed

and ductile-to-brittle transition mechanism for workpiece material in ultra-high speed machining, Int. J. Mech. Sci. 104 (2015) 44-59.

[15] P. Simon, A. Beaucamp, P. Charlton, Brittle - ductile transition in shape adaptive grinding (SAG) // Frontiers in Optics (2016).

[16] G. Xiao, S. To, G. Zhang, Molecular dynamics modelling of brittle–ductile cutting mode transition: Case study on silicon carbide, Int. J. Mach. Tool Manu. 88 (2015) 214-222.

[17] J. Jacob, Determination of the ductile to brittle transition and critical depth of cut in 6H-silicon carbide through fly cutting, https://www.researchgate.net, 2014 (accessed 2014-4-09)

[18] H. Toshihiko, K. Tomokazu, H. Atsushi, Surface roughness control based on digital copy milling concept to achieve autonomous milling operation, Procedia CIRP 4(4) (2012) 35-40.

[19] M. Zhou, X. J. Wang, B. K. A. Ngoi, J. G. K. Gan, Brittle - ductile transition in the diamond cutting of glasses with the aid of ultrasonic vibration, J. Mater. Process. Tech. 121(2-3) (2002) 243-251.

[20] G. H. Campbell, B. J. Dalgleish, A. G. Evans, Brittle-to-ductile transition in silicon carbide, J Am. Ceram. Soc. 72(8) (2010) 1402-1408.

[21] D. B. Marshall, B. R. Lawn, Indentation of brittle materials, Micro indentation Technology in Materials Science and Engineering 1 (1985) 889.

[22] L. D. Zhang, Theoretical and experimental studies on the ultra-precision face-milling of engineering Ceramics, Hebei University of Technology, Tianjin, 2002.

[23] S. Malkin, Grinding technology: theory and applications of machining with abrasives, SME, 1989.

[24] O. Scattergood, N. Blake, Ductile-regime machining of germanium and silicon, J Am. Ceram. Soc. 73(4) (1990) 949-957.

[25] M. Arif, M. Rahman, W. Y. San, Analytical model to determine the critical conditions for the modes of material removal in the milling process of brittle material, J. Mater. Process. Tech. 212(9) (2012) 1925-1933.

[26] T. Hiroaki, S. Shoichi, Damage-free machining of monocrystalline silicon carbide, CIRP Ann-Manuf. Techn. 62(1) (2013) 55-58.

[27] Y. Qiao, A. S. Argon, Brittle-to-ductile fracture transition in fe–3wt.%si single crystals by thermal crack arrest, Mech. Mater. 35(9) (2003) 903-912.

Figures

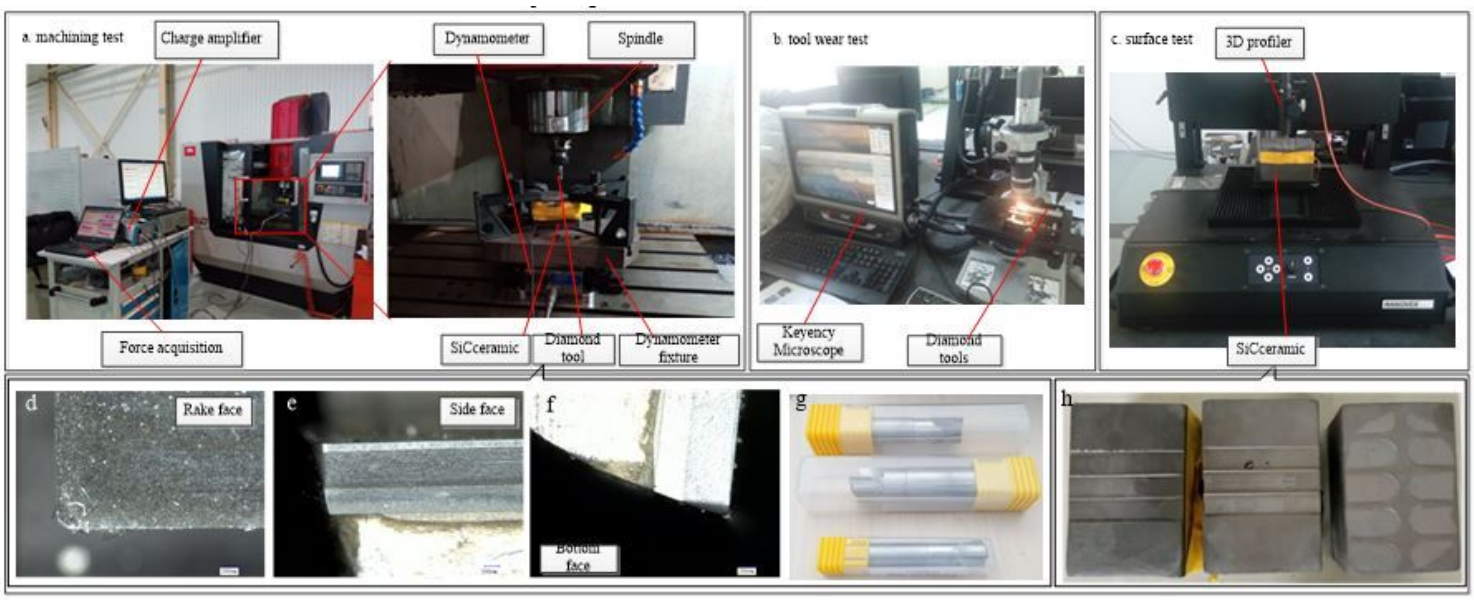

Figure 1

Test of SiC Ceramics milling (a. machining test; b. tool wear test; c. surface tests; def. rake, side, and bottom faces of new tool; g. diamond tool; h. SiC workpiece)

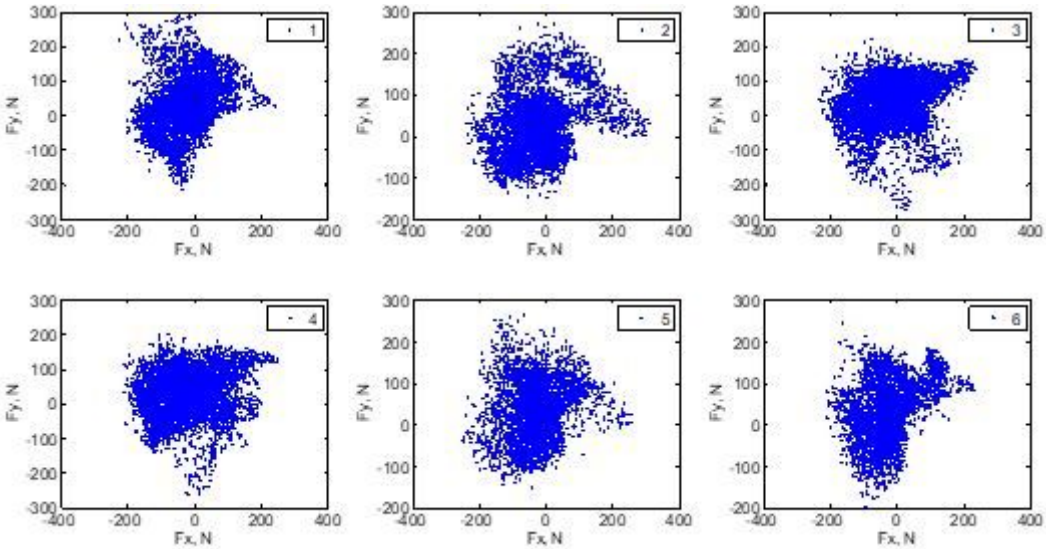

Figure 2

X-Y plot of cutting forces

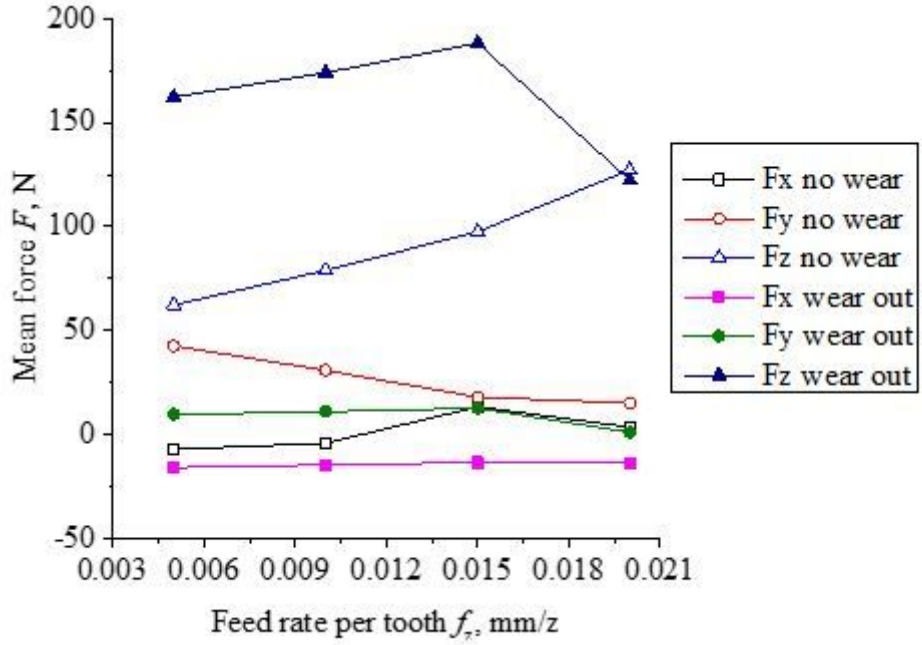

Figure 3

Cutting forces distribution in varied feed milling with the same parameter before and after tool wear

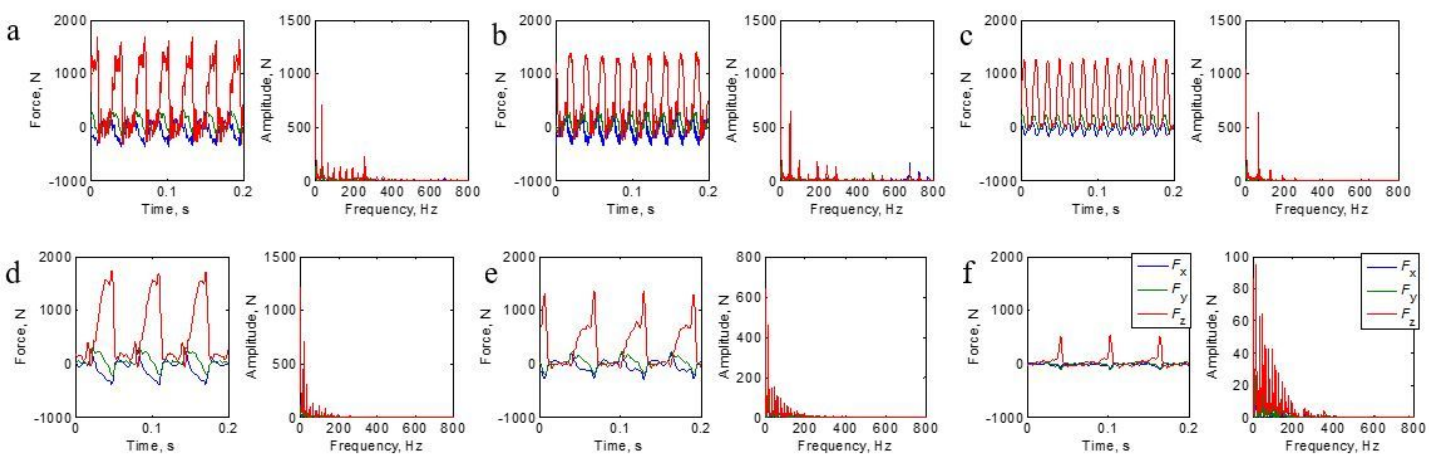

Figure 4

Time and frequency domain signals of cutting forces of worn tool. (a) n=2000 r/min, fz=0.01 mm/z, ap=0.15 mm. (b) n=3000 r/min, fz=0.01 mm/z, ap=0.15 mm. (c) n=4000 r/min, fz=0.01 mm/z, ap=0.15 mm. (d) ap=0.2 mm, n=1000 r/min, fz=0.01 mm/z. (e) ap=0.15 mm, n=1000 r/min, fz=0.01 mm/z. (f) ap=0.1 mm, n=1000 r/min, fz=0.01 mm/z.

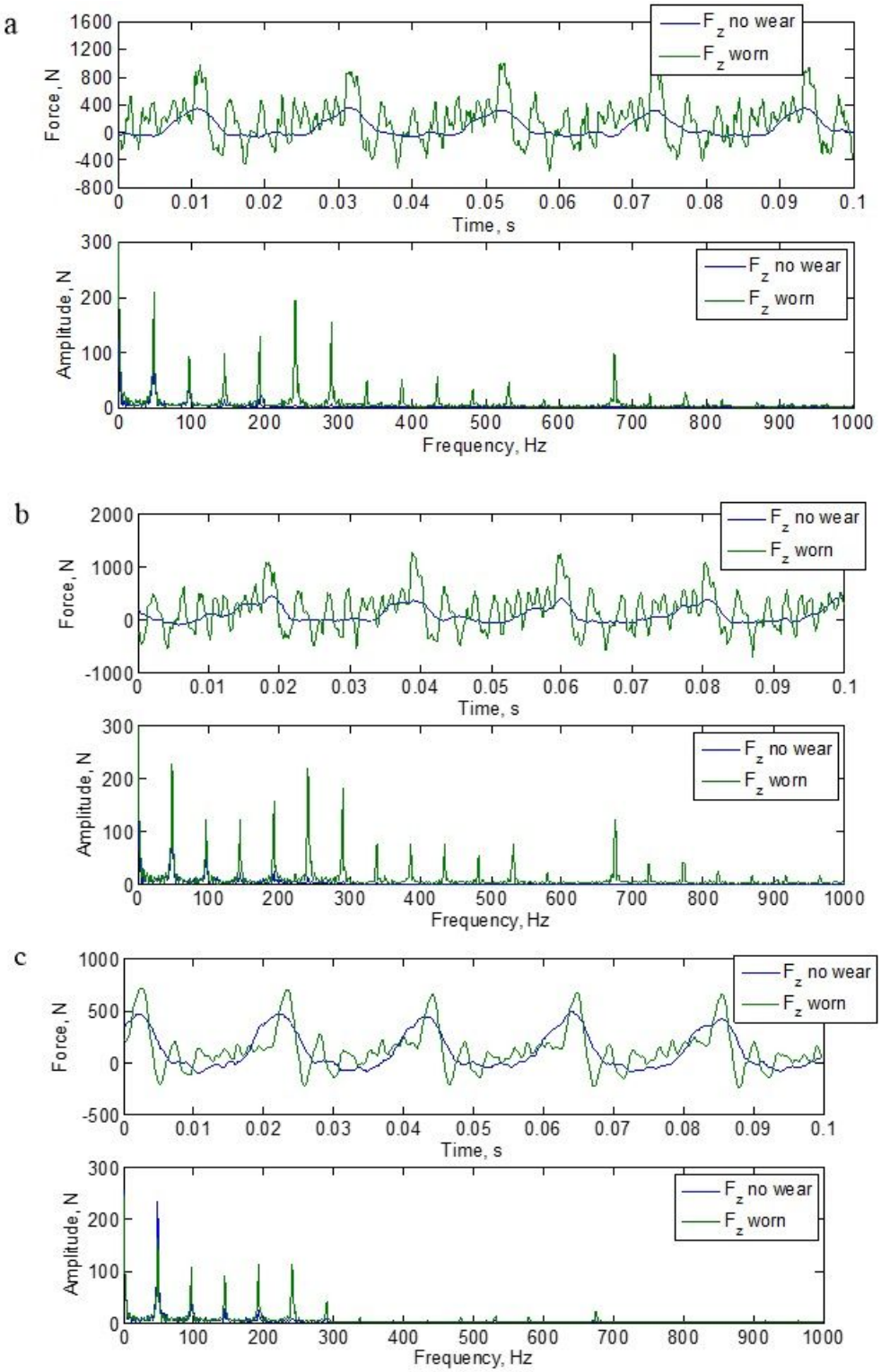

Figure 5

Force signals before and after tool wear in varied feed rate cutting (n=3000 r/min, ap=0.1 mm). (a) fz=0.005 mm/z. (b) fz=0.015 mm/z. (c) fz=0.02 mm/z.

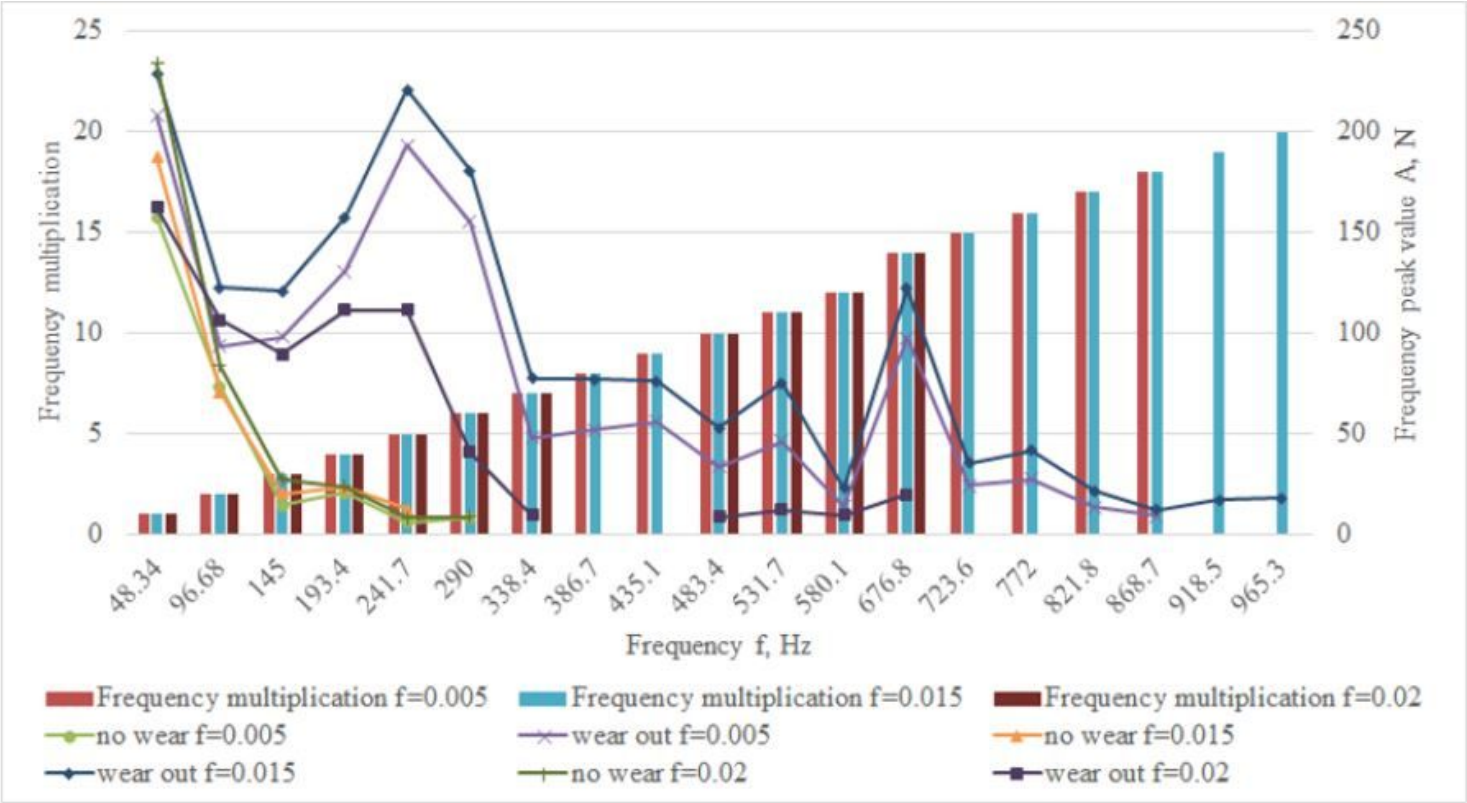

Figure 6

Force rotation frequency of tool before and after wear

Figure 7

Tool surfaces. New tool. (a) Rake face 100×. (b) Flank face 100×. (c) Bottom edge 100×. Worn tool. (d) Rake face 50×. (e) Flank face 20×. (f) Bottom face 50×.

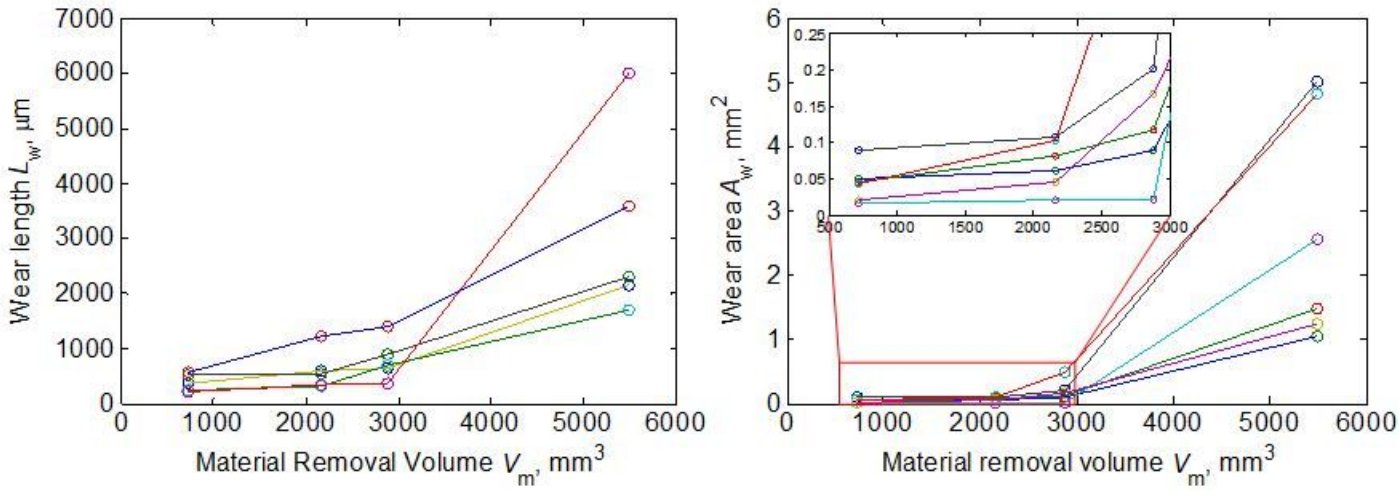

Figure 8

Tool wear length and wear area with material removal volume

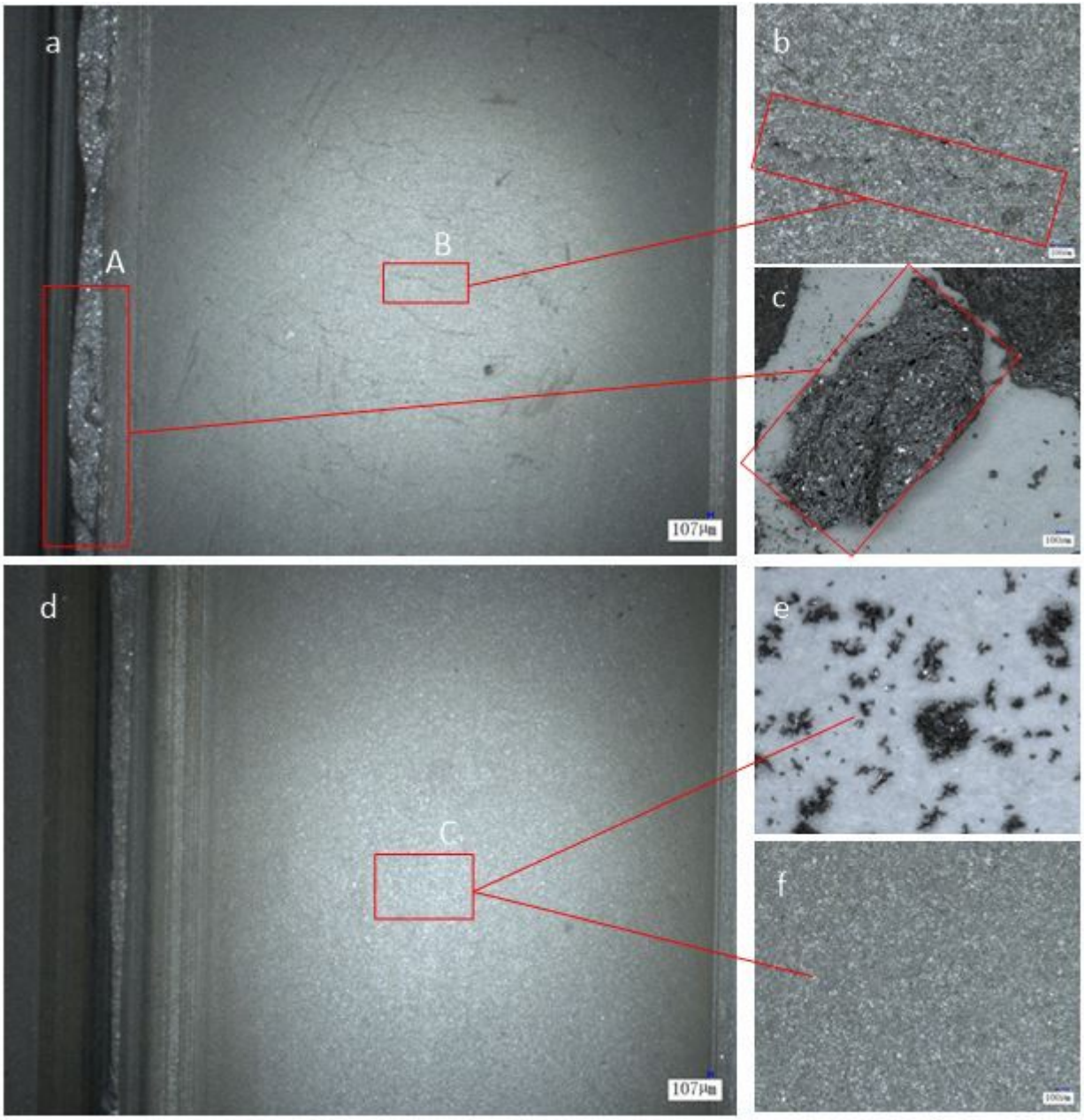

Figure 9

Surface integrity. (abc) poor quality surface with material spalling induced by crack (n=1000 r/min fz=0.01 mm/z ap=0.2 mm). (def) high quality surface (n=3000 r/min fz=0.015 mm/z ap=0.1 mm)

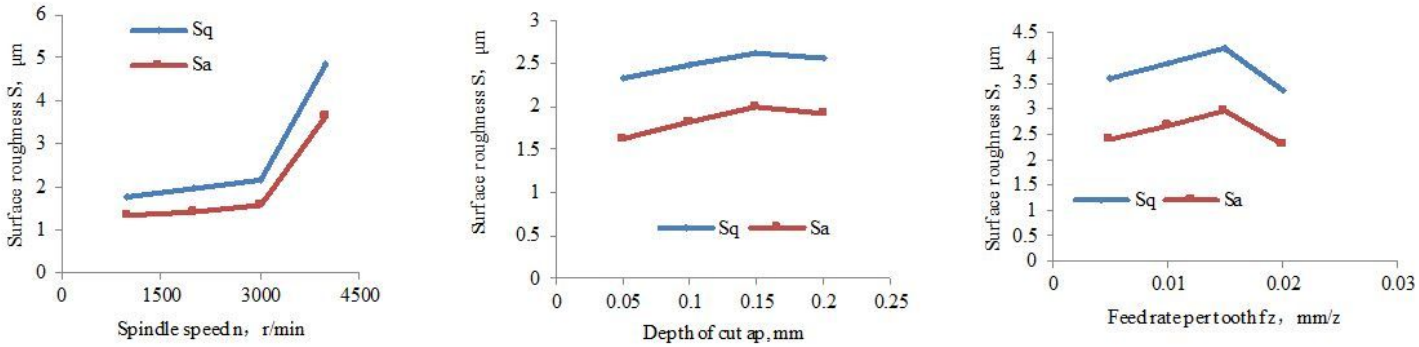

Figure 10

Surface roughness Sa and Sq obtained by (a)varied speed test (fz=0.01 mm/z, ap=0.15 mm). (b) varied cutting depth test(n=1000 r/min and fz=0.01). (c) varied feed test (n=3000 r/min and ap=0.1).

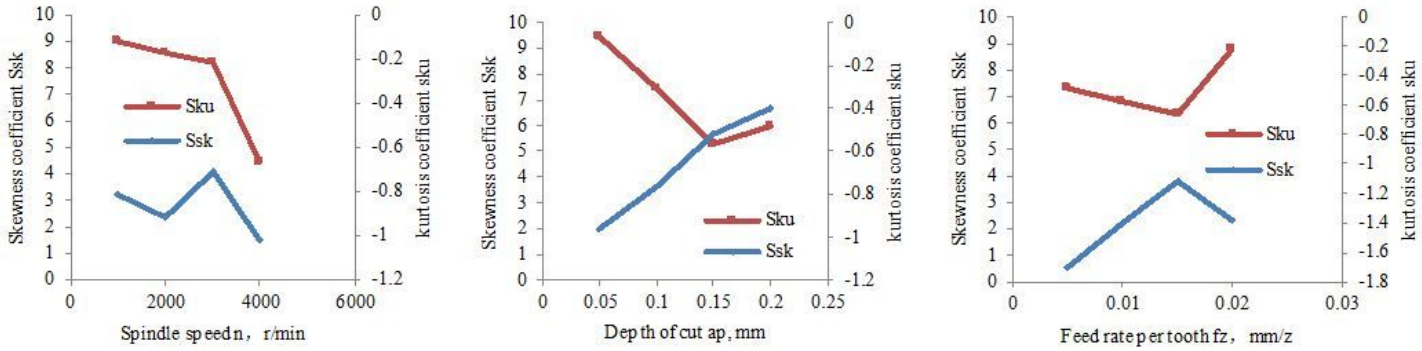

Figure 11

Surface skewness coefficient Ssk and kurtosis coefficient Sku obtained by (a)varied speed (fz=0.01 mm/z, ap=0.15 mm). (b) varied cutting depth (n=1000 r/min and fz=0.01). (c) varied feed (n=3000 r/min and ap=0.1).

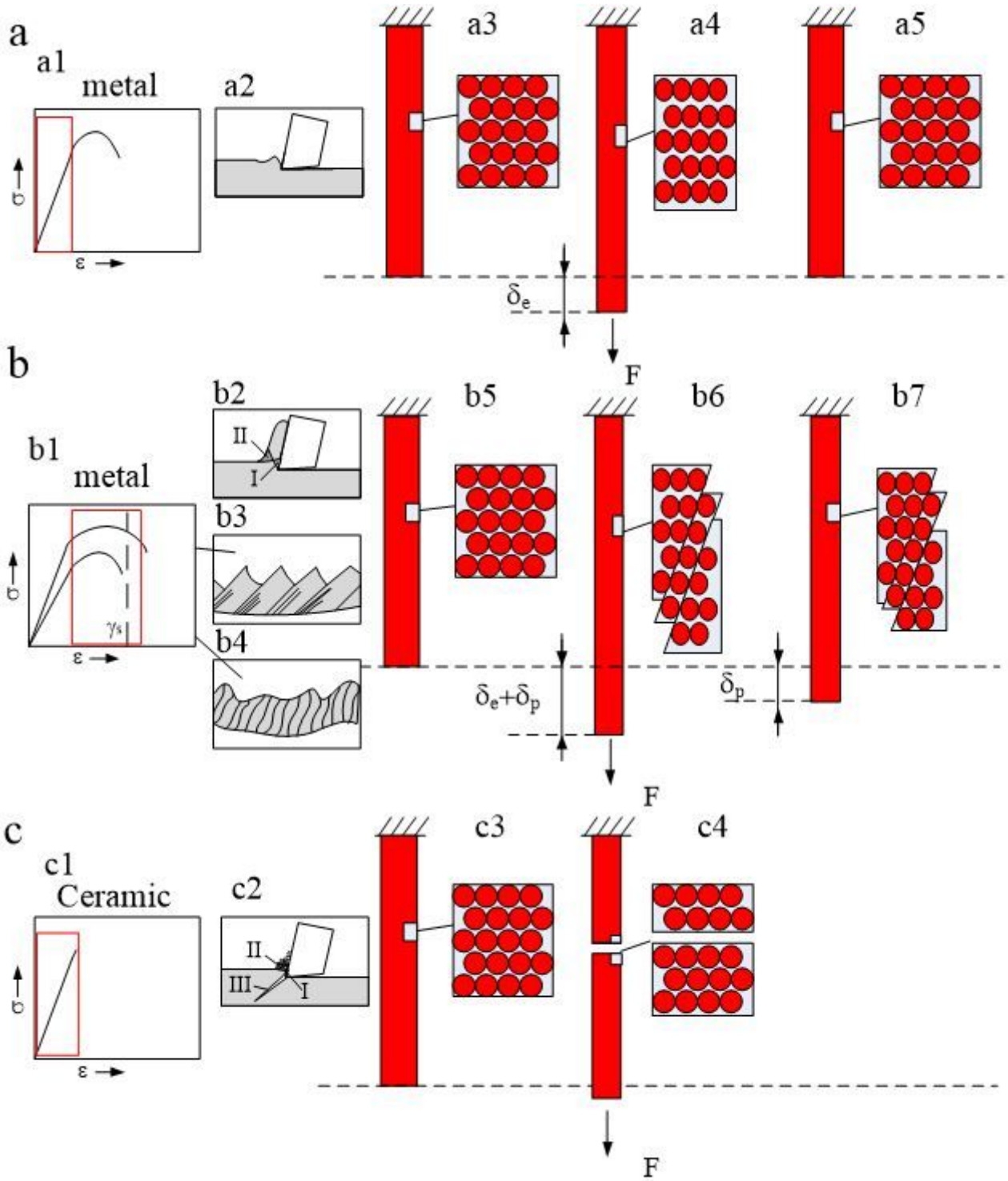

Figure 12

Chip formation mechanisms and stress-stain comparison of metal and ceramics. (a) elastic deformation of metal. (b) plastic deformation of metal. (c) brittle deformation of ceramics. (F is force, δe and δp are the elastic deformation and plastic deformation.)

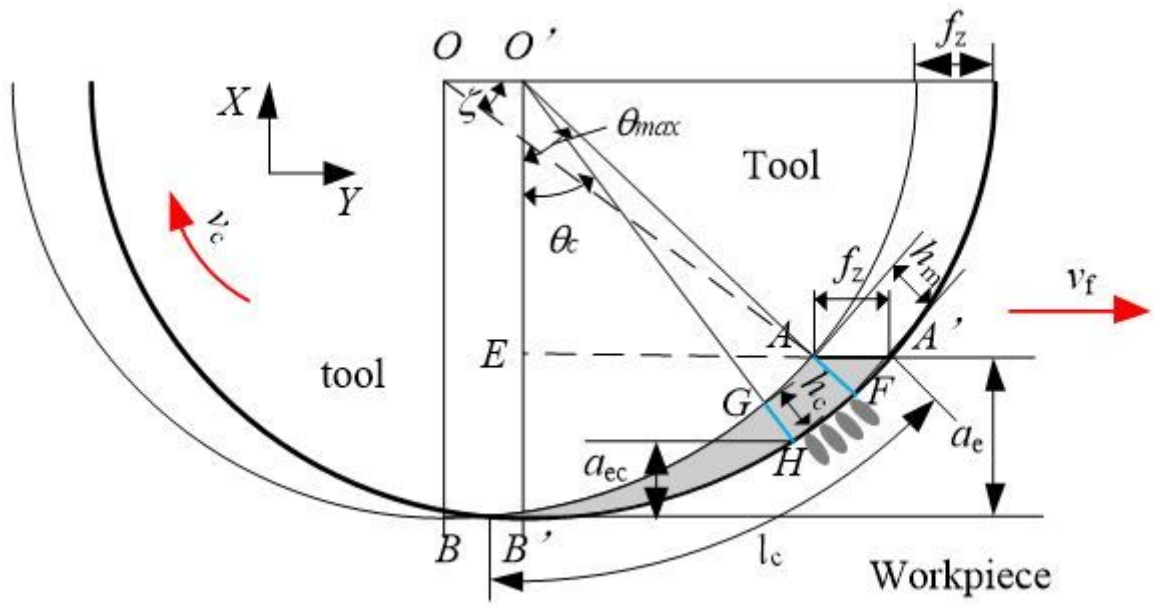

Figure 13

Milling geometry model

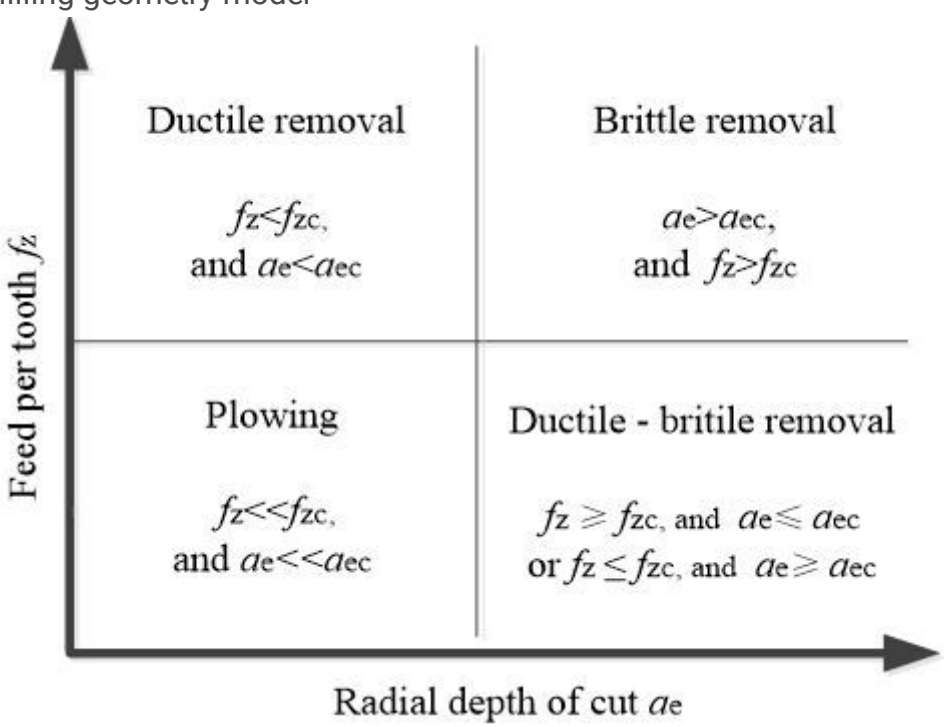

Figure 14

Critical condition of brittle-ductile cutting transition